The induction of atherogenic dyslipidaemia in poloxamer 407-treated mice is not mediated through PPARα

Thomas P. Johnston and David J. Waxman

Abstract

The copolymer surfactant poloxamer 407 (P-407) has been used to induce a dose-controlled dyslipidaemia in both mice and rats. Human macrophages cultured with P-407 exhibit a concentration-dependent reduction in cholesterol efflux to apolipoprotein A1 (apoA1) due to down-regulation of the ATP-binding cassette transporter A1 (ABCA1). Peroxisome proliferator-activated receptor alpha (PPARα) can increase expression of liver X receptor alpha (LXRα) in macrophages and thereby promote the expression of ABCA1, which, in turn, mediates cholesterol efflux to apoA1. This study investigated point(s) along this signalling pathway at which P-407 might act to inhibit cholesterol efflux from macrophages. A transactivation assay was used to evaluate whether P-407 could either activate PPARα or block the activation of PPARα by an established PPARα agonist. P-407 was also evaluated for its potential to alter plasma lipid concentrations following its administration to both normal C57BL/6 and PPARα-deficient mice. P-407 was unable to modulate PPARα activity, as determined in cell-based transactivation assays. Moreover, P-407-induced dyslipidaemia occurred at the same rate and to the same extent in PPARα-deficient mice as was observed in C57BL/6 mice, suggesting no role for PPARα in P-407-mediated dyslipidaemia. Although PPARs are known to mediate the transcriptional regulation of the two major apolipoproteins associated with HDL (apoA1 and apoA2), P-407 treatment resulted in a similar decrease (~30%) in the plasma concentration of apoA1 in both control and PPARα-deficient mice. Since our previous work demonstrated that P-407 was unable to abrogate the capacity of a known LXRα agonist to increase cholesterol efflux from macrophages, P-407 is likely to exert its effect, either directly or indirectly, on ABCA1, rather than on LXRα. On the basis of these findings it is concluded that PPARα does not mediate the P-407-dependent reduction in apoA1-facilitated cholesterol efflux from macrophages.

Division of Pharmaceutical Science, School of Pharmacy, University of Missouri-Kansas City, Kansas City, MO, USA

Thomas P. Johnston

Division of Cell and Molecular Biology, Department of Biology, Boston University, Boston, MA, USA

David J. Waxman

Correspondence: T. P. Johnston, Division of Pharmaceutical Sciences, Rm. 211A, School of Pharmacy, University of Missouri-Kansas City, 5005 Rockhill Road, Kansas City, MO 64110-2499, USA. E-mail: johnstont@umkc.edu

Introduction

Peroxisome proliferator-activated receptors (PPARs) are nuclear receptors that, upon heterodimerization with retinoid X receptor (RXR), function as ligand-activated transcriptional regulators of genes controlling lipid and glucose metabolism (Pineda et al 1999). PPARα, which is activated by fibrates, fatty acids and eicosanoids (Chinetti et al 2000a), is highly expressed in liver, heart, muscle and kidney, but is also present in cells of the arterial wall, including monocytes, macrophages, macrophage foam cells, smooth muscle and endothelial cells (Chinetti et al 2000a). PPARα has a role in macrophage lipid homoeostasis and cholesterol efflux, which is the first step in the reverse cholesterol transport pathway. In macrophages, PPARα activators induce the expression of the scavenger receptor CLA-1/SR-BI, which binds HDL with high affinity (Chinetti et al 2000b). In addition, in differentiated macrophages and macrophage-derived foam cells, PPARα activators induce ATP-binding cassette transporter A1 (ABCA1) gene expression through their inductive effects on the expression of liver X receptor alpha (LXRα) and promote cholesterol efflux to apolipoprotein (apo) A1 (Chinetti et al 2001).

Recently, we reported how a polymeric chemical compound known as poloxamer 407 (P-407) affected cholesterol homoeostasis in primary human monocyte-derived macrophages (Johnston et al 2006). P-407 is a triblock copolymer comprised of repeating poly(oxyethylene) and poly(oxypropylene) units and is normally used as a surfactant. However, our laboratory

has utilized P-407 to develop a murine model of dose-controlled atherogenic dyslipidaemia (elevated plasma triglyceride (TG) with a simultaneous reduction in high-density lipoprotein (HDL) cholesterol) (Johnston 2004; Leon et al 2006). Administration of P-407 to mice for 16 weeks results in the formation of aortic fibrofatty lesions comparable in size and number with those formed using classic diet-induced and gene-knockout mouse models of atherogenesis (Palmer et al 1998; Leon et al 2006). Because this model is routinely utilized by numerous laboratories throughout the world, we continue to explore the mechanisms responsible for the atherogenic dyslipidaemia produced in this model, as well as any changes that may occur in cell lipid, insulin and glucose homoeostasis. Examples of how researchers use this model include: determining how the pharmacokinetics of specific drugs are altered in the context of atherogenic dyslipidaemia (Brocks et al 2006); determining the immune response to oxidized LDL-cholesterol produced in this model (Johnston & Zhou 2007); determining how the dyslipidaemic state affects key enzymes of lipid metabolism (e.g., endothelial lipase) (T. Ishida et al 2007, personal communication); and determining the hepatic production rate of triglycerides (Millar et al 2005). Thus, it is critical to develop a better understanding of the mechanisms behind the cell lipid, enzyme and gene signalling pathways altered by P-407 in this mouse model of atherogenic dyslipidaemia. Recently, we demonstrated both a significant reduction in the expression of ABCA1 and, as a result, apoA1-mediated cholesterol efflux, when macrophages were cultured with P-407 (Johnston et al 2006). Interestingly, although PPARα activation reduces the cholesteryl ester:free cholesterol (CE:FC) ratio in macrophages by inhibiting acyl-CoA:cholesterol acyltransferase (ACAT), which, in turn, inhibits cellular CE formation (Chinetti et al 2003), we observed an increase in the values of the CE:FC ratio in liver and in eight peripheral tissues in P-407-treated rats (Johnston et al 2006). Even more intriguing is our finding that neither hepatic microsomal ACAT activity nor hepatic ACAT2 protein expression is altered in P-407-treated mice (Leon et al 2006). Therefore, it is important to determine whether P-407, either directly or indirectly, perturbs PPARα activity in a manner that could help explain the increased CE levels seen in tissues of P-407-treated rats (Johnston et al 2006), and whether any such modulation of PPARα activity might contribute to the atherogenic dyslipidaemia observed in P-407-treated mice.

Previous key findings include: a concentration-dependent decrease in, firstly, ABCA1 gene expression and, secondly, cholesterol efflux in macrophages treated with P-407 (Johnston et al 2006); an increase in the CE:FC ratio determined for liver and eight peripheral tissues in P-407-treated rats (Johnston et al 2006); and no effect of P-407 on ACAT protein and activity levels (Leon et al 2006). On the basis of these earlier findings, we sought to investigate the potential for P-407 to modulate PPARα activity, as determined in a cell-based transactivation assay. Additionally, we evaluated whether the atherogenic dyslipidaemia in mice treated with P-407 was dependent on PPARα, as determined using a PPARα-deficient mouse model. Lastly, in addition to their role in peroxisome proliferation in rodents, PPARs are also involved in the control of HDL-cholesterol levels based, in part, on PPAR-mediated transcriptional regulation of the major apolipoproteins,

apoA1 and apoA2 (Schoonjans et al 1996). Since it is well established that apoA1, rather than apoA2, confers HDL's anti-atherogenic effect, we also assessed whether there was any change in the concentration of apoA1, relative to apoE, in plasma obtained from P-407-treated mice.

Materials and Methods

Materials

Wy-14,643 was obtained from Sigma Chemical Co. (St Louis, MO, USA). Male PPARα-knockout mice, ~18 g, were purchased from the Jackson Laboratory (strain name = 129S4/SvJae-Ppara^{tm1Gonz}/J). Plasmids were obtained from the same sources as previously reported (Maloney & Waxman 1999; Shipley & Waxman 2004; Shipley et al 2004).

Transactivation assay

The transactivation assay described previously (Maloney & Waxman 1999; Shipley & Waxman 2004; Shipley et al 2004) was used to assess the effect of P-407 on PPARα transcriptional activity. Briefly, COS-1 cells (American Type Culture Collection, Rockville, MD, USA) were passaged in 100-mm tissue culture dishes (Greiner Labortechnik, Germany) in DMEM supplemented with 10% fetal bovine serum (FBS) (Gibco, Grand Island, NY) and 50 U mL^{-1} penicillin/streptomycin (Gibco). Cells were cultured overnight at 37°C and then reseeded at 2000–4000 cells/well in a 96-well tissue culture plate (Greiner Labortechnik) in DMEM containing 10% FBS. The cells were grown for 24 h and then transfected as described previously (Chang & Waxman 2005), using FuGENE 6 transfection reagent (Roche Diagnostics Corp., Indianapolis, IN, USA). Previous studies indicated little or no significant endogenous PPARα activity in these cells (Maloney & Waxman 1999). Twenty-four hours after P-407 treatment, cells were washed once in cold phosphate-buffered saline (PBS) (pH 7.4), and then lysed by incubation at 4°C in passive cell lysis buffer for 15–30 min (Promega). Firefly and Renilla luciferase activity was measured in the cell lysate using the Dual Luciferase Activity Kit (Promega).

In-vivo experiments

Three groups of mice (n = 6 mice per group) were used to assess whether PPARα played a role in P-407-mediated dyslipidaemia in mice. Group 1 consisted of B6 mice treated with P-407 (0.5 g kg^{-1}), while Groups 2 and 3 consisted of PPARα-knockout mice treated with either normal saline or P-407 (0.5 g kg^{-1}), respectively. To reduce animal numbers, we utilized our previously-reported literature values of plasma lipid concentrations obtained following the administration of saline to B6 mice (Group 4 mice). After intraperitoneal administration of 0.5 mL of either normal saline or P-407 (dissolved in normal saline), blood samples (50 μL) were obtained from each mouse by tail-vein sampling at 0, 2, 4, 8, 16 and 24 h post-dosing. All blood samples were collected into heparinized tubes, the plasma obtained, and the samples

stored at −80°C until the time of lipid analysis. All procedures for P-407 administration and subsequent blood collection were in accordance with the institution's guide for the care and use of laboratory animals, and the treatment protocol was approved by the Institutional Animal Care and Use Committee (IACUC) at the University of Missouri-Kansas City.

Plasma samples were analysed for total cholesterol (Allain et al 1974) and triglycerides (Bucolo & David 1973) using standard enzymatic, colorimetric assay kits. The concentration of HDL-cholesterol was determined by first precipitating the VLDL and LDL fractions with a phosphotungstic acid/magnesium solution (Bachorik & Albers 1986) and then analysing the supernatant obtained after centrifugation at $10000\,g$ for total cholesterol. Non-HDL-cholesterol was simply calculated as total cholesterol minus HDL-cholesterol.

Apolipoprotein analysis

ApoA1 in plasma was measured by an apoA1 ELISA assay (Dansky et al 1999). Rabbit anti-mouse apoA1 (Biodesign, Saco, ME, USA) was purified on protein A affinity columns (Pierce) and a sample was biotinylated (Amersham). Purified antibody, diluted 1:400 in bicarbonate buffer, was applied to wells of Nunc Maxisorb ELISA plates and incubated overnight at 4°C. All subsequent incubations were performed at room temperature with gentle agitation. Wells were washed with PBS and blocked with casein blocker (Pierce) for 1 h, followed by addition of plasma and serum standards for 2 h. Serum standards were calibrated by comparing with purified mouse apoA1. Plates were washed with PBS/Tween (0.5%) and biotinylated antibodies, diluted 1:250 in PBS/Tween, were applied for 2 h. After washing, streptavidin/horseradish peroridase (HRP) (Pierce) was applied for 1 h. HRP enzyme was detected by incubation with TurboTMB substrate (Pierce). The reaction was terminated with $1\,\textsc{m}$ sulfuric acid, and the absorbance was measured at 450 nm on a model 450 microplate reader (Bio-Rad, Richmond, CA, USA).

A similar ELISA assay was used to quantify the plasma concentrations of apoE (Wahrle et al 2004). Briefly, rabbit anti-mouse apoE (Biodesign) was purified on protein A affinity columns (Pierce) and then applied (0.5 μg/well) to 96-well plates overnight. Plates were then washed with PBS, blocked with 1% milk in PBS, and then washed again. Plasma samples were diluted directly into 0.1% bovine serum albumin, 0.025% Tween in PBS. Standards were based on pooled plasma from B6 mice containing approximately $70\,\mu g\,mL^{-1}$ apoE. Following a 2-h sample incubation, the plate was washed and 3 μg/well of biotinylated goat anti-apoE (Calbiochem, catalogue No. 178479) was added. The antibody was biotinylated using a biotin-maleimide reagent (Vector Laboratories, Burlingame, CA, USA). After incubation of the secondary antibody (2 h), the plate was washed and poly-HRP streptavidin (Pierce) was added at 1:6000 and incubated for 1 h. The plate was washed, developed with tetramethylbenzidine (Sigma), and read at 650 nm.

Data analysis

Luciferase activity values were normalized for transfection efficiency by dividing the measured Firefly luciferase activity values by the Renilla luciferase activity obtained for the same cell extract (i.e. (Firefly/Renilla) × 1000). Data is presented as the mean ± standard deviation luciferase activity for n = 3 separate determinations. Data obtained from the transactivation assays was assessed for statistical significance, relative to vehicle controls, by using a one-way analysis of variance. Post-hoc analysis of individual differences between treatment groups was assessed using the method of Scheffe, with $P < 0.05$ deemed significant.

Data acquired from the in-vivo experiments were processed in the following manner. The increased plasma total cholesterol and HDL-cholesterol seen in PPARα-deficient mice (Peters et al 1997) was taken into account before comparing the plasma lipid-vs-time profiles for PPARα-deficient mice to the corresponding profiles for B6 mice. Using plasma total cholesterol concentrations for P-407-treated PPARα-deficient mice and P-407-treated B6 mice as an example, the average increase in the plasma concentration of total cholesterol for saline-treated, PPARα-deficient mice, relative to saline-treated B6 mice (~106 mg dL^{-1}; see lower two curves in Figure 3A), was subtracted from each plasma total cholesterol concentration for the P-407-treated PPARα-deficient mice. The resulting values were then compared with the cholesterol concentrations at each time point for the P-407-treated, B6 mice. A similar procedure was followed for comparing plasma concentrations of HDL-cholesterol. The unpaired Student's t-test was used for comparing plasma lipid concentrations at each time point between genotypes (PPARα-deficient vs B6) for a given treatment (P-407 or saline), as well as for comparing corresponding plasma lipid concentrations at each time point between treatments (P-407 vs saline) within a given genotype (PPARα-deficient or B6). A value of $P < 0.05$ was deemed statistically significant. Values used for the lipid and lipoprotein plasma concentrations for saline-treated B6 mice (Group 4) were those reported previously (Palmer et al 1998; Johnston et al 1999). Mean values of the plasma concentrations of apoA1 and apoE were processed in the same manner as plasma total and HDL-cholesterol concentrations described above.

Results

Transactivation assay

A cell-based transactivation assay was used to investigate whether P-407 directly modulates PPARα activity. Treatment of cells with P-407 at concentrations ranging from 50 nM to 200 μM did not increase the transcriptional activity of either mouse PPARα or human PPARα relative to vehicle (Figure 1 A, B). Moreover, P-407 did not inhibit human PPARα transcriptional activity stimulated by the PPARα agonist Wy-14,643 (Figure 2).

PPARα-deficient mouse experiments

In B6 mice, plasma total cholesterol increased from a baseline value of 78 mg dL^{-1} to 693 mg dL^{-1} by 24 h after administration of P-407 (Figure 3A). The P-407-induced increase was evident as early as 4 h ($P < 0.05$). Administration of P-407
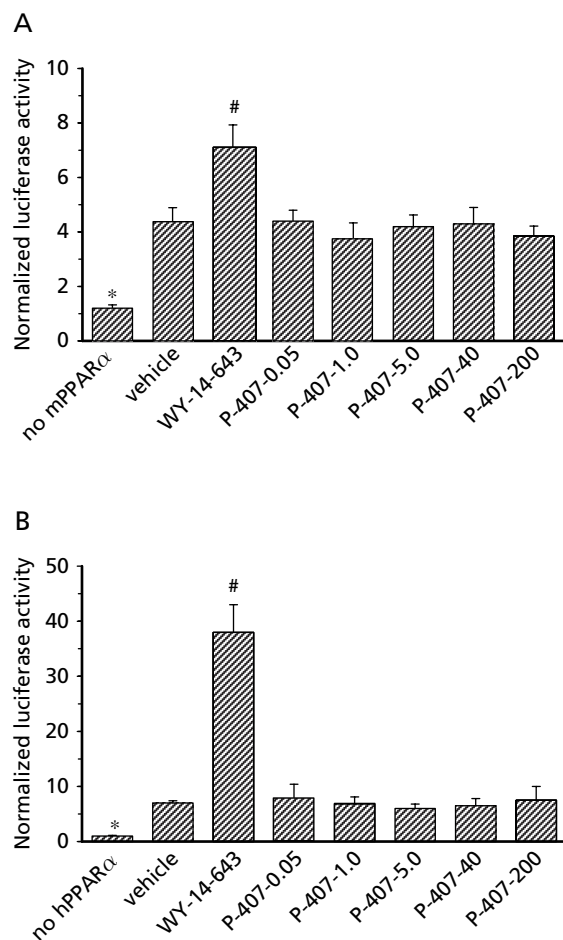
Figure 1 The effect of P-407 on mouse (A) and human (B) PPARα activity in-vitro. All P-407 concentrations are in μM. Data represents the mean ± s.d., n = 3. First bar, no PPARα control; second bar, cells transfected with either mouse (A) or human (B) PPARα expression plasmid and then treated with vehicle. The increase in activity of this sample compared with bar 1 reflects activation of PPARα by cellular fatty acids and other endogenous activators. Bars 3–8 are the same as bar 2, except that the cells were stimulated for 24 h with either Wy-14,643 or P-407 at the micromolar concentrations indicated. *P < 0.05, bar 1 (no PPARα) vs all other bars; #P < 0.05, bar 3 (WY-14-643) vs all other bars.

Figure 2 The effect of P-407 on human PPARα activity stimulated by the PPARα-activator, Wy-14-643. All P-407 concentrations are in μM. Data represents the mean ± s.d. *P < 0.05, bars 1 (no PPARα) and 2 (vehicle) vs all other bars; #P < 0.05, bar 2 (vehicle) vs bar 1 (no PPARα).

to PPARα-deficient mice produced a similar time-course in the plasma concentration of total cholesterol, although the profile was situated above the concentration–time profile obtained with the P-407-treated B6 mice. This reflects the increase in plasma concentrations of HDL-cholesterol and total cholesterol that characterize PPARα-deficient mice (Peters et al 1997) (also see two lower curves in Figure 3A). When this increase in the plasma total cholesterol was taken into account, no significant difference in the plasma total cholesterol profile was observed in P-407-treated, PPARα-deficient mice when compared with P-407-treated B6 mice.

The plasma concentration–time profiles for non-HDL cholesterol (calculated) and plasma TG are depicted in Figure 3B and 3C, respectively. There was no significant difference between the non-HDL cholesterol concentration–time profiles
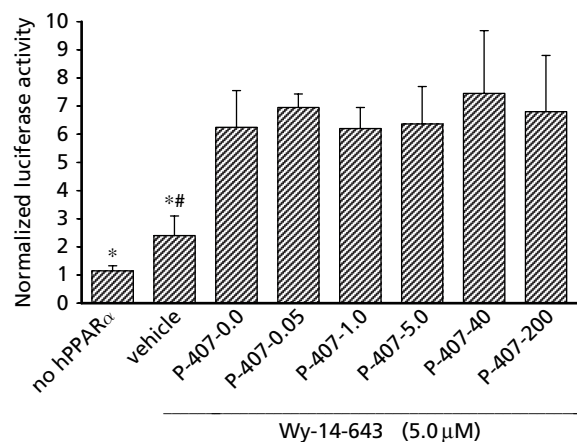
for P-407-treated B6 and P-407-treated PPARα-deficient mice (Figure 3B). However, as with the plasma total cholesterol concentration–time profiles, there was a significant (P < 0.05) difference between the profiles of the P-407-treated B6 mice and P-407-treated PPARα-deficient mice when each profile was individually compared with its respective saline control. These same trends can be observed in Figure 3C with regard to the plasma TG concentration–time profiles.

Figure 3D illustrates the plasma HDL concentration–time profiles resulting from the administration of either P-407 or saline to B6 and PPARα-deficient mice. Again, disruption of the gene for PPARα causes a greater baseline plasma HDL-cholesterol concentration (Peters et al 1997) in saline-treated PPARα-deficient mice than for saline-treated B6 mice. Baseline plasma HDL concentrations were ~100 mg dL⁻¹ for PPARα-deficient mice, compared with ~60 mg dL⁻¹ for B6 mice. Administration of P-407 to both B6 and PPARα-deficient mice resulted in a gradual, but steady, increase in plasma HDL concentrations throughout the duration of the experiment (Figure 3D). With the P-407-induced mouse model of atherogenic dyslipidaemia, plasma HDL concentrations increase slightly following P-407 administration, but most of the cholesterol is found in the LDL and VLDL fractions, rather than in the HDL fraction. The slight, but gradual, rise in the plasma HDL-cholesterol concentration for 24 h post-dosing reflects increased cholesterol synthesis (Johnston & Palmer 1997; Johnston 2004; Leon et al 2006), although the ratio of plasma HDL-cholesterol:non-HDL-cholesterol concentrations in P-407-treated mice typically range from 3.5 at time 0 h (before injection) to 0.2 at 24 h (i.e., the time point at which maximum plasma lipid concentrations are attained in this model following a single injection of P-407) (Johnston 2004).

As with the other plasma lipid concentration vs time profiles, all plasma HDL-cholesterol concentrations for P-407-treated mice (both B6 and PPARα-deficient) were significantly greater (P < 0.05) than the corresponding HDL-cholesterol concentrations for their respective saline-injected controls beginning at 4 h post-dosing. However, there was no
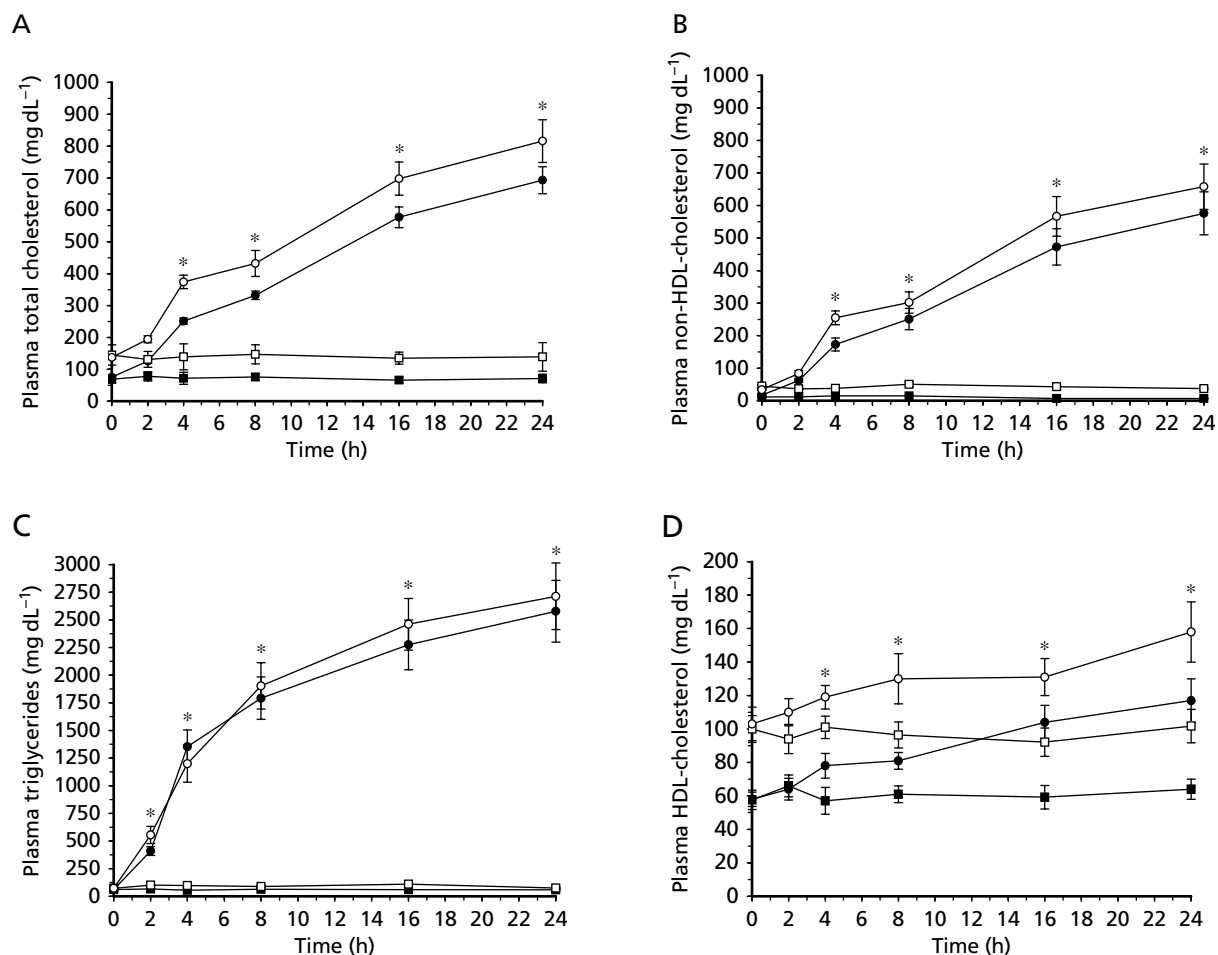
Figure 3 Plasma total cholesterol (A), non-HDL-cholesterol (B), triglycerides (C) and HDL-cholesterol (D) concentrations following administration of normal saline (squares) to either C57BL/6 (closed squares) or PPARα-deficient (open squares) mice and P-407 (0.5 gkg^{-1}) (circles) to either C57BL/6 (closed circles) or PPARα-deficient (open circles) mice. Data represents the mean ± s.d. *$P < 0.05$, plasma concentrations for P-407-treated mice (both B6 and PPARα-deficient) vs corresponding concentrations for their respective saline-injected controls beginning at 4 h (2 h for triglycerides). However, there was no significant difference in plasma lipid concentrations between P-407-treated B6 and P-407-treated PPARα-deficient mice when concentrations for the latter group were normalized for changes induced by the gene knockout as described in Materials and Methods. Similarly, there was no significant difference in plasma lipid concentrations between saline-treated B6 and saline-treated PPARα-deficient mice when concentrations for the latter group were normalized for changes induced by the gene knockout as described in Materials and Methods.

significant difference in plasma HDL-cholesterol concentrations between B6 and PPARα-deficient mice when each group was administered P-407 (Figure 3D). The same trend was observed when both B6 and PPARα-deficient mice were administered saline (Figure 3D).

Plasma apolipoprotein analysis

Because atherogenesis is well-documented in apoE-deficient mice and both apoA1 and apoE have been shown to function as cholesterol acceptors and thereby facilitate cholesterol efflux from macrophages (Joyce et al 2002), we analysed plasma for both apoA1 and apoE. P-407 decreased the plasma concentration of apoA1 to a similar extent (30 to 32%; $P < 0.05$) in both B6 and PPARα-deficient mice (Table 1). In contrast, the plasma concentration of apoE increased slightly, but, not significantly ($P > 0.05$), in both B6 and PPARα-deficient mice administered P-407.

Table 1 The effect of acute P-407 administration on plasma apolipoprotein concentration

Genotype/treatment	apoA1 (mgdL^{-1})	apoE (mgdL^{-1})
B6/saline	82.0 ± 4.7	2.6 ± 0.3
B6/P-407	57.4 ± 3.2*	2.9 ± 0.2
PPARα$^{-/-}$/saline	136 ± 11.9	2.8 ± 0.3
PPARα$^{-/-}$/P-407	92.7 ± 8.6*	3.2 ± 0.2

Values are mean ± s.d. 24 h after P-407 administration; *$P < 0.05$, compared with saline-injected control.

Discussion

Previous work had demonstrated that P-407 treatment significantly decreased cholesterol efflux from macrophages by

down-regulating ABCA1 gene expression, and that P-407 did not abrogate the action of a known LXRα agonist to stimulate apoA1-mediated cholesterol efflux from macrophages (Johnston et al 2006). In this study, we investigated whether P-407 modulated PPARα activity with the goal of extending our work to the PPAR–LXR–ABCA1 signalling pathway and to further elucidate the mechanism(s) responsible for reduced cellular cholesterol efflux along this pathway, as well as the dyslipidaemia observed in this murine model of atherogenesis (Johnston 2004).

Using a transactivation assay, we determined that P-407 was unable to activate the transcriptional activity of either mouse or human PPARα. Furthermore, P-407 did not inhibit a known PPARα agonist from activating human PPARα. To ascertain whether PPARα played a role in P-407-mediated dyslipidaemia, we compared the effects of P-407 treatment in wild-type (B6) and PPARα-deficient mice. It was critical to evaluate P-407 for its potential to mediate dyslipidaemia in PPARα-deficient mice, since a compound's ability to modulate PPARα is not always predicted from the results of an in-vitro transactivation assay (Peters et al 1996). After taking into consideration the increase in plasma HDL-cholesterol and, consequently, total cholesterol, seen in PPARα-deficient mice, there were no significant differences in P-407-induced plasma concentration–time profiles of total cholesterol, HDL-cholesterol, non-HDL-cholesterol (calculated) and TG. Therefore, these data strongly support the conclusion that neither P-407, nor some intermediate that results from the administration of P-407, is functioning as a PPARα agonist in-vivo, similar to the action of fibrate drugs described below.

Assessment of anti-atherogenic activity of PPARα agonists in rodent models of atherosclerosis is hampered by the fact that, firstly, rodents develop a pro-inflammatory peroxisome proliferative response in the liver and, secondly, classical animal models, such as the LDL-receptor or apoE-deficient mice, display an aberrant hyperlipidaemic response to the fibrate class of hypolipidaemic drugs (Marx et al 2004). As an example of the latter, several studies have evaluated the use of fibrates (PPARα agonists) in several rodent models. Duez et al (2002) reported that even though administration of fenofibrate to $apoE^{-/-}$ mice at a dose of $100\,mg\,kg^{-1}$ daily for 8 weeks resulted in a significant increase in both plasma total cholesterol and triglycerides, there was a reduction in atherosclerosis. Similarly, Fu et al (2003) reported that ciprofibrate markedly increased the plasma levels of atherogenic lipoproteins in $apoE^{-/-}$ mice; however, in contrast to Duez et al (2002), this investigator reported a significant enhancement in the development of atherosclerosis. Clearly, the ability of fibrate drugs to increase plasma lipids in mice is well established, although their capacity to inhibit atherosclerosis is still controversial. Notably, the effects of fibrates in rodents are opposite to that observed clinically. Activation of PPARα with fibrate drugs in man increases fatty acid oxidation, decreases very-low-density lipoprotein (VLDL), increases lipolysis and increases HDL-cholesterol and reverse cholesterol transport. These actions result in a decrease in plasma TG, a decrease in plasma small, dense, atherogenic LDL-cholesterol and an increase in HDL-cholesterol (Marx et al 2004).

ApoA1, the major cholesterol acceptor of HDL, is induced by fibrates in man, but is decreased by fibrates in rodents (Duez et al 2005). This is because HDL metabolism is regulated in an opposite fashion by fibrates in rodents (decrease) and man (increase) due to sequence divergences in the respective apoA1 promoters (Ngoc et al 1998). Consequently, in rats, fibrates, such as fenofibrate and clofibrate, significantly decrease plasma apoA1, apoA2 and apoE concentrations (Staels et al 1992), whereas, in mice, fibrates cause a decrease in the plasma concentration of apoA1, but an increase in apoA2 (Duez et al 2005). In this study, P-407 caused a reduction in the plasma concentration of apoA1 in treated mice. Since it is primarily apoA1 that confers the atheroprotective effects of HDL, this may help explain why mice develop aortic atherosclerotic lesions after 16 weeks of P-407 administration (Palmer et al 1998; Johnston 2004). Simultaneously, there was a slight increase in the plasma concentration of apoE. Interestingly, we previously demonstrated that HDL isolated from the plasma of P-407-treated mice contained more apoE, relative to apoA1 (Johnston et al 1999).

The decrease in plasma apoA1 following P-407 administration is not likely to be mediated by PPARα since, firstly, P-407 was unable to directly modulate the activity of mouse PPARα using a transactivation assay and, secondly, the atherogenic dyslipidaemia that occurs following administration of P-407 to mice was not mediated through PPARα. Therefore, as it relates to apolipoproteins, even though P-407 treatment caused a reduction in the plasma concentration of apoA1, similar to the fibrates, we conclude that P-407 did not function as a PPARα agonist. Instead, we suggest that P-407, by significantly reducing ABCA1 gene expression, contributes, in part, to induction of an atherogenic plasma lipid profile. Indeed, Joyce et al (2002) demonstrated that overexpression of ABCA1 in C57BL/6 mice resulted in a unique anti-atherogenic profile characterized by decreased plasma cholesterol, cholesteryl esters, free cholesterol, non-HDL cholesterol and apoB, but markedly increased HDL, apoA1 and apoE. In contrast, administration of P-407 to C57BL/6 mice results in an atherogenic profile characterized by increased plasma total cholesterol, triglycerides and non-HDL cholesterol, but markedly decreases HDL-cholesterol and apoA1. The fact that P-407 induced this same type of atherogenic profile in PPARα-deficient mice provides further evidence that the observed reduction in plasma apoA1 levels, which resulted from the administration of P-407, was not mediated through PPARα, and that P-407 was not functioning as a PPARα agonist.

Conclusion

In conclusion, as it pertains to the PPAR–LXR–ABCA1 signalling pathway, our findings suggest that acute administration of P-407 to mice does not modulate the activity of PPARα and, hence, the reduced cholesterol efflux we previously observed when macrophages were treated with P-407 (Johnston et al 2006) most likely results from P-407's direct inhibitory effect on ABCA1 gene expression. Additionally, the atherogenic dyslipidaemia that occurs following P-407 administration to mice, as well as the decrease in the plasma concentration of apoA1, appears not to be regulated by P-407's effect(s) at the level of PPARα. Future research will focus on whether the protein expression of ABCA1 is also modulated following P-407 administration.

References

Allain, C. A., Poor, L. S., Chan, C. S., Richmond, W., Fu, P. C. (1974) Enzymatic determination of total serum cholesterol. *Clin. Chem.* **20**: 470–476

Bachorik, P. S., Albers, J. J. (1986) Precipitation methods for quantitation of lipoproteins. *Methods Enzymol.* **129**: 78–100

Brocks, D. R., Ala, S., Aliabadi, H. M. (2006) The effect of increased lipoprotein levels on the pharmacokinetics of cyclosporine A in the laboratory rat. *Biopharm. Drug Dispos.* **27**: 7–16

Bucolo, G., David, H. (1973) Quantitative determination of serum triglycerides by the use of enzymes. *Clin. Chem.* **19**: 476–479

Chang, T. K., Waxman, D. J. (2005) Pregnane X receptor-mediated transcription. *Methods Enzymol.* **400**: 588–598

Chinetti, G., Fruchart, J. C., Staels, B. (2000a) Peroxisome proliferators-activated receptors (PPARs): nuclear receptors at the crossroads between lipid metabolism and inflammation. *Inflamm. Res.* **49**: 497–505

Chinetti, G., Gbaguidi, G. F., Griglio, S., Mallat, Z., Antonucci, M., Poulain, P., Chapman, J., Fruchart, J. C., Tedgui, A., Najib-Fruchart, J., Staels, B. (2000b) CLA-1/SR-BI is expressed in atherosclerotic lesion macrophages and regulated by activations of peroxisome proliferator-activated receptors. *Circulation* **101**: 2411–2417

Chinetti, G., Lestavel, S., Bocher, V., Remaley, A. T., Neve, B., Pineda, T. I., Tessier, E., Minnich, A., Jaye, M., Duverger, N., Brewer, B. H., Fruchart, J. C., Clavey, V., Staels, B. (2001) PPARα and PPARγ activators induce cholesterol removal from human macrophage foam cells through stimulation of the ABCA1 pathway. *Nat. Med.* **7**: 53–58

Chinetti, G., Lestavel, S., Fruchart, J. C., Clavey, V., Staels, B. (2003) Peroxisome proliferator-activated receptor α reduces cholesterol esterification in macrophages. *Circ. Res.* **92**: 212–217

Dansky, H. M., Charlton, S. A., Sikes, J. L., Heath, S. C., Simantov, R., Levin, L. F., Shu, P., Moore, K. J., Breslow, J. L., Smith, J. D. (1999) Genetic background determines the extent of atherosclerosis in apoE-deficient mice. *Arterioscler. Thromb. Vasc. Biol.* **19**: 1960–1968

Duez, H., Chao, Y. S., Hernandez, M., Torpier, G., Poulain, P., Mundt, S., Mallat, Z., Teissier, E., Burton, C. A., Tedgui, A., Fruchart, J. C., Fievet, C., Wright, S. D., Staels, B. (2002) Reduction of atherosclerosis by the peroxisome proliferator-activated receptor α agonist fenofibrate in mice. *J. Biol. Chem.* **277**: 48051–48057

Duez, H., Lefebvre, B., Poulain, P., Torra, I. P., Percevault, F., Luc, G., Peters, J. M., Gonzalez, F. J., Gineste, R., Helleboid, S., Dzavik, V., Fruchart, J. C., Fievet, C., Lefebvre, P., Staels, B. (2005) Regulation of human apoAI by gemfibrozil and fenofibrate through selective peroxisome proliferator-activated receptor alpha modulation. *Arterioscler. Thromb. Vasc. Biol.* **25**: 585–591

Fu, T., Kashireddy, P., Borensztajn, J. (2003) The peroxisome-proliferator-activated receptor α agonist ciprofibrate severely aggravates hypercholesterolemia and accelerates the development of atherosclerosis in mice lacking apolipoprotein E. *Biochem. J.* **373**: 941–947

Johnston, T. P. (2004) The P-407-induced murine model of dose-controlled hyperlipidemia and atherosclerosis: a review of findings to date. *J. Cardiovasc. Pharmacol.* **43**: 595–606

Johnston, T. P., Palmer, W. K. (1997) Effect of poloxamer 407 on the activity of microsomal 3-hydroxy-3-methylglutaryl CoA reductase in rats. *J. Cardiovasc. Pharmacol.* **29**: 580–585

Johnston, T. P., Zhou, X. (2007) Oxidation of low-density lipoprotein cholesterol following administration of poloxamer 407 to mice results from an indirect effect. *J. Cardiovasc. Pharmacol.* **49**: 246–252

Johnston, T. P., Baker, J. C., Jamal, A. S., Hall, D. D., Emeson, E. E., Palmer, W. K. (1999) Potential downregulation of HMG-CoA reductase after prolonged administration of P-407 in C57BL/6 mice. *J. Cardiovasc. Pharmacol.* **34**: 831–842

Johnston, T. P., Jaye, M., Webb, C. L., Krawiec, J. A., Alom-Ruiz, S. P., Sachs-Barrable, K., Wasan, K. M. (2006) Poloxamer 407 (P-407)-mediated reduction in the gene expression of ATP-binding-cassette transporter A1 may contribute to increased cholesterol in peripheral tissues of P-407-treated rats. *Eur. J. Pharmacol.* **536**: 232–240

Joyce, C. W., Amar, M. J. A., Lambert, G., Vaisman, B. L., Paigen, B., Najib-Fruchart, J., Hoyt, R. F., Neufeld, E. D., Remaley, A. T., Fredrickson, D. S., Brewer, H. B., Santamarina-Fojo, S. (2002) The ATP binding cassette transporter A1 (ABCA1) modulates the development of aortic atherosclerosis in C57BL/6 and apoE-knockout mice. *Proc. Natl Acad. Sci. USA* **99**: 407–412

Leon, C., Wasan, K. M., Sachs-Barrable, K., Johnston, T. P. (2006) Acute P-407 administration to mice causes hypercholesterolemia by inducing cholesterolgenesis and down-regulating low-density lipoprotein receptor expression. *Pharm. Res.* **23**: 1597–1607

Maloney, E. K., Waxman, D. J. (1999) *trans*-activation of PPARα and PPARγ by structurally diverse environmental chemicals. *Toxicol. Appl. Pharmacol.* **161**: 209–218

Marx, N., Duez, H., Fruchart, J. C., Staels, B. (2004) Peroxisome proliferator-activated receptors and atherogenesis: regulators of gene expression in vascular cells. *Circ. Res.* **94**: 1168–1178

Millar, J. S., Cromley, D. A., McCoy, M. G., Rader, D. J., Billheimer, J. T. (2005) Determining hepatic triglyceride production in mice: comparison of poloxamer 407 with Triton WR-1339. *J. Lipid Res.* **46**: 2023–2028

Ngoc, V. D., Chopin-Delannoy, S., Gervois, P., Bonnelye, E., Martin, G., Fruchart, J., Laudet, V., Staels, B. (1998) The nuclear receptors peroxisome proliferator-activated receptor α and Rev-erbα mediate the species-specific regulation of apolipoprotein A-I expression by fibrates. *J. Biol. Chem.* **273**: 25713–25720

Palmer, W. K., Emeson, E. E., Johnston, T. P. (1998) Poloxamer 407-induced atherogenesis in the C57BL/6 mouse. *Atherosclerosis* **136**: 115–123

Peters, J. M., Zhou, Y. C., Ram, P. A., Lee, S. S., Gonzalez, F. J., Waxman, D. J. (1996) Peroxisome proliferator-activated receptor alpha required for gene induction by dehydroepiandrosterone-3 beta-sulfate. *Mol. Pharmacol.* **50**: 67–74

Peters, J. M., Hennuyer, N., Staels, B., Fruchart, J. C., Fievet, C., Gonzalez, F. J., Auwerx, J. (1997) Alterations in lipoprotein metabolism in peroxisome proliferator-activated receptor alpha-deficient mice. *J. Biol. Chem.* **272**: 27307–27312

Pineda, T. I., Gervois, P., Staels, B. (1999) Peroxisome proliferator-activated receptor alpha in metabolic disease, inflammation, atherosclerosis, and aging. *Curr. Opin. Lipidol.* **10**: 151–159

Schoonjans, K., Staels, B., Auwerx, J. (1996) The peroxisome proliferator activated receptors (PPARs) and their effects on lipid metabolism and adipocyte differentiation. *Biochim. Biophys. Acta* **1302**: 93–109

Shipley, J. M., Waxman, D. J. (2004) Simultaneous, bidirectional inhibitory crosstalk between PPAR and STAT5b. *Toxicol. Appl. Pharmacol.* **199**: 275–284

Shipley, J. M., Hurst, C. H., Tanaka, S. S., DeRoos, F. L., Butenhoff, J. L., Seacat, A. M., Waxman, D. J. (2004) *trans*-activation of PPARα and induction of PPARα target genes by perfluorooctane-based chemicals. *Toxicol. Sci.* **80**: 151–160

Staels, B., van Tol, A., Andreu, T., Auwerx, J. (1992) Fibrates influence the expression of genes involved in lipoprotein metabolism in a tissue-selective manner in the rat. *Arterioscler. Thromb.* **12**: 286–294

Wahrle, S. E., Jiang, H., Parsadanian, M., Legleiter, J., Han, X., Fryer, J. D., Kowalewski, T., Holtzman, D. M. (2004) ABCA1 is required for normal central nervous system apoE levels and for lipidation of astrocyte-secreted apoE. *J. Biol. Chem.* **279**: 40987–40993